Jpn. J. Appl. Phys. Vol. 38 (1999) pp. 1832–1834
Part 1, No. 3B, March 1999

Magnetic Domain Pinning in Lithographically Patterned Amorphous Magnetic Layer

Jong-Ching WU[1], Ying-Wen HUANG[1], Bing-Mau CHEN[3], Te-ho WU[2] and Han-Ping D. SHIEH[3]
[1]*Deptartment of Physics, National Changhua University of Education, Changhua, Taiwan 500, R.O.C.*
[2]*Department of Humanities and Sciences, National Yunlin University of Science and Technology, Touliu, Taiwan 640, R.O.C*
[3]*Institute of Electro-Optic Engineering., National Chiao-tung University, Hsinchu, Taiwan 300, R.O.C.*

(Received October 14, 1998; accepted for publication December 7, 1998)

Artificial pinning sites have been fabricated for the magnetic domain pinning in perpendicular anisotropy magneto-optical (MO) thin film media. The pinning sites were radial hole array made by patterning a layer of radial gold grid on the silicon nitride (SiN) coated silicon (Si) substrate using a standard electron beam lithography. Various magnetization and demagnetization procedures were performed to investigate the magnetic domain pinning behavior. A polar Kerr microscope was used in situ to monitor the magnetic wall motion and a magnetic force microscope was employed to scan the magnetic domain structures. Magnetic domains were found to be pinned inside the hole array and resembled to the geometric shape of the holes. The coercivity in the patterned MO layer is much higher than in the unpatterned MO layer. Moreover, the coercivity in the larger pinning sites area is higher than in the smaller pinning sites area.

KEYWORDS: magnetic domain pinning, magneto-optical, radial hole array, electron beam lithography, Kerr microscope, magnetic force microscope

1. Introduction

The strong demanding of ultrahigh data storage density has attracted intensive studies on the recording media. Among the research, besides searching new materials and read/write techniques, one inevitable effort has been devoted to make the size of every single recording bit smaller. Recently, large area discrete submicron patterned dot array of magneto-optical (MO) media has been realized using laser interference lithography,[1,2] however the roughness of the dot edges suffered from the etching damage has been indicated to be a problem in making recorded domain stable.[3–5] One way to overcome the problem is to provide artificial pinning sites in the continuous magnetic films as originally proposed by Gadetsky *et al.*,[6] in which a photolithography was used. In carrying the idea but for the sake of higher data storage density, we have shown denser and smaller pinning domains by using electron beam lithography,[7,8] in which the artificial pinning sites were made in the hole array of polymethyl methacrylate (PMMA). PMMA, however, has certain deficiencies such as it peels off from the substrate easily, which is resulted from cracking during the sputtering of MO film. In this paper, we present a better way as to provide a patterned gold structure instead of PMMA for pinning the magnetic domains and the corresponding of pattern geometry to the domain structures is discussed

2. Sample Preparation and Image Observation

The sample fabrication consisted of two steps: the fabrication of artificial pinning sites, which is made of radial gold grid; and the sputtering of MO recording media, which is an amorphous $Dy_{23.5}(FeCo)_{76.5}$ film. The pre-formatted gold grids were made using electron beam lithography. An electron resist, PMMA, was spun onto a SiN-coated Si-wafer and was baked at 140°C overnight, and electron beam lithography[9] was used to delineate a variety of submicron pinning sites such as radial hole array and square-, donut-, and star-shaped hole array. Following resist development, 30 nm thick of gold was thermally deposited and the patterns were transferred onto the substrate by a lift-off procedure. The MO active layer $Dy_{23.5}(FeCo)_{76.5}$ with thickness of 50 nm was DC magnetron co-sputtered onto the pre-formatted pinning patterns, and a 30 nm thick of SiN layer was subsequently deposited to protect the MO layer. The final layer structure is: Si/SiN (200 nm)/$Dy_{23.5}(FeCo)_{76.5}$ (50 nm)/SiN (30 nm) in the holes and Si/SiN (200 nm)/gold (30 nm)/$Dy_{23.5}(FeCo)_{76.5}$ (50 nm)/SiN (30 nm) on the ridges. For the magnetic domain observation, first of all, a polar Kerr microscope equipped with an up to 9 kOe of electromagnet was used in situ to monitor the magnetic domain wall motion across the pinning sites. Then, during the various states of magnetization or demagnetization the sample was moved to a magnetic force microscope (MFM) for scanning the images of magnetic domain structures as well as the morphology of the patterned structures. A Digital Instruments Nanoscope IIIa MFM equipped with phase extender[10] was used in this study. The magnetic tip with a CoCr-coated Si tip magnetized along the tip axis was used to scan the magnetic domain structures in tapping-lift mode.[11]

3. Results and Discussions

The patterned sample was first imaged at the state of as deposited before exposing to the external magnetic field and the magnetic image hardly showed any structures. Then, before the MFM imaging the samples were either magnetized or demagnetized in external magnetic fields perpendicular or parallel to the film plane in order for the investigation of domain pinning behavior. In order to know the field strength as to better control the domain reversal, the coercivity of unpatterned sample (with the same layer structures of the patterned sample but no pre-formatted gold grid) was identified to be about 6.69 kOe in this material by adopting extraordinary Hall effect measurement. Figure 1(a) shows the morphology of the radial gold grid, while Fig. 1(b) to (f) show the corresponding magnetic domain images in the various states of magnetization and demagnetization as described below. First, an extremely high magnetic field, 26 kOe, was applied perpendicular to the film plane for magnetization. Thus, the magnetic moment of the sample was saturated in one direction, out of plane, as shown in the MFM image of Fig. 1(b). That the ridges show broader in magnetic image than in morphology is due to the natural divergence of the magnetic filed. Apparently, the magnetic domains were pinned inside the radial hole array and resembled the geometric shapes of the radial

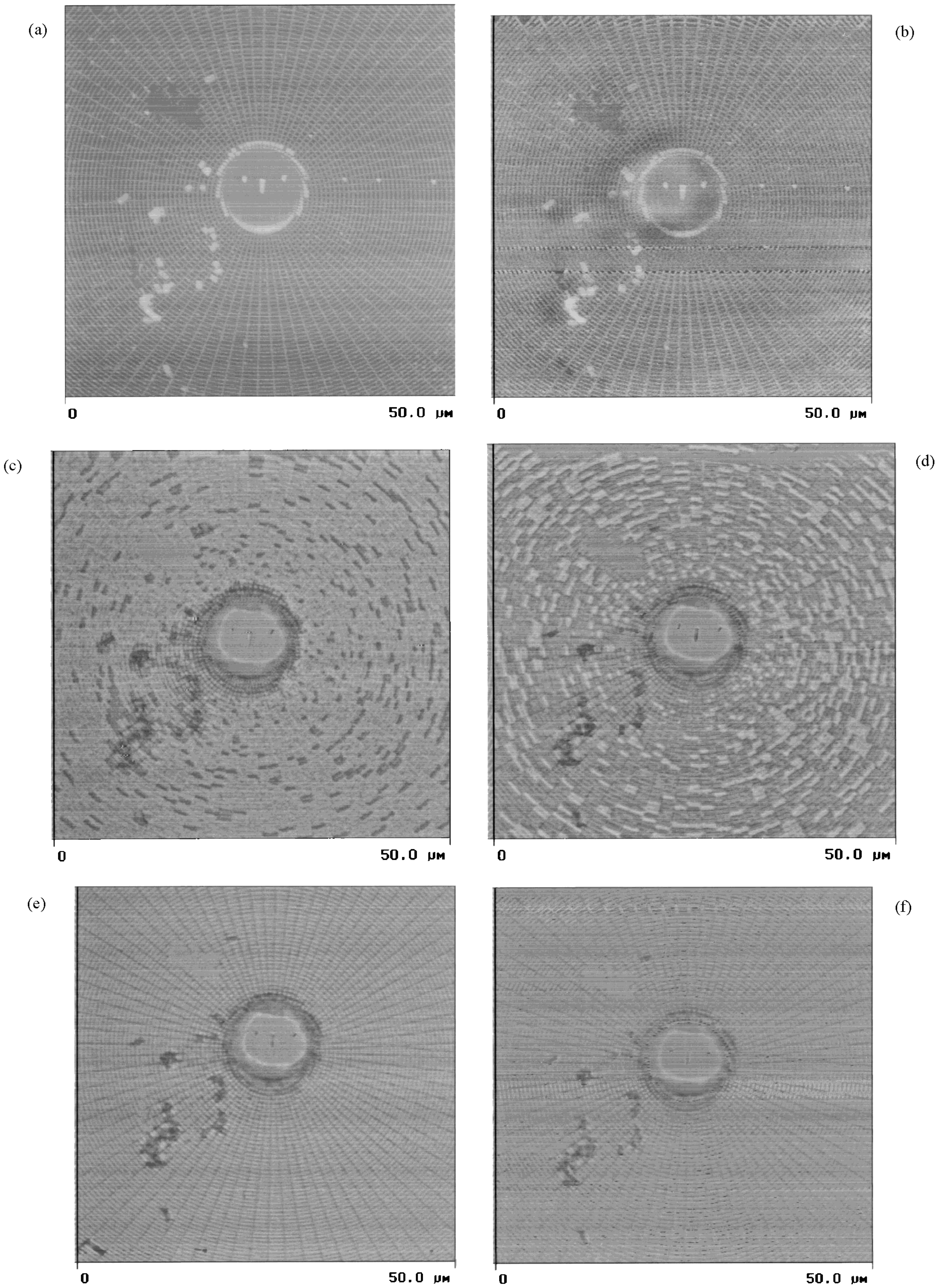

Fig. 1. Morphology of the patterned MO layer and the corresponding magnetic domain images under various states of magnetization and demagnetization. (a) is the AFM image of the radial hole array. (b) is the MFM image taken after the sample was magnetized with 26 kOe applied in out of plane direction. (c), (d), and (e) are the MFM images taken after the external magnetic field was applied opposite to the previous magnetization direction and the magnetic field were turned off at 6.93 kOe, 8.86 kOe, and 12 kOe, respectively. Note that the contrast was offset to be much higher for better images, i.e. the darker areas represent the pinned domains reversed from the previously magnetized image (b). Apparently, (e) and (b) possess completely opposite contrast. (f) is the MFM image taken after 26 kOe applied in the film plane.

gold grid. Same results were found in the other shapes of hole arrays. Subsequently, the sample was moved to a polar Kerr microscope for the direct observation of domain reversal, in which the external magnetic field was applied opposite to the direction of previous magnetization. As the magnetic field was increased to approach near the coercivity of the unpatterned sample, the reversed domains started to nucleate outside the patterned MO layer. In addition, the pinned domains started to reverse from the smaller pinning sites, which is in the inner parts. Once the domain reversal was taking place across the patterned MO layer, the external magnetic field was turned off and the sample was moved to MFM for image scans. Figure 1(c) shows the MFM image taken after the external magnetic field was turned off at 6.93 kOe, in which only few pinned domains were reversed. Notice that besides the domains were all reversed outside the patterned area (not shown) one can only see some complete domain reversal (discrete dot array) close to the central ring area. Furthermore, as the external magnetic field was kept increasing higher, more magnetic domains were reversed as shown in the MFM image of Fig. 1(d), in which the external magnetic field was turned off at 8.86 kOe. The magnetic field up to 9 kOe under Kerr microscope wasn't high enough to reverse all the pinned domains. Therefore, an independent electromagnet having highest magnetic field of 26 kOe was used for further studies without direct observation of the domain reversal (for the first magnetization also). Care was taken as to ensure the direction of the previous magnetic field applied. In addition, the magnetic field was turned off frequently for MFM image scans while the field was kept increasing. Consequently, the complete domain reversal was found to take place at about 12 kOe of external magnetic field, as shown in the MFM image of Fig. 1(e). Note that the contrast of Fig. 1(e) is completely opposite to Fig. 1(b). Since the MFM tip was magnetized along the tip axis and was kept at the same magnetization configuration during the entire MFM image scans, this result indicates that the MFM contrast is indeed associated with the up- and down-magnetized domains. Figure 1(f) is the MFM image taken after the sample was demagnetized by an external magnetic field of 26 kOe applied in the film plane, in which the MFM signal is weaker. A quantitative analysis concerning the anisotropy coercivity in this patterned MO layer will be published elsewhere.

4. Conclusions

We have developed a technique of using pre-formatted gold structures, superior to the previous PMMA method,[7,8] for the studies of the magnetic domain pinning behavior. The pinning mechanism is believed to be the combination vector effect of perpendicular magnetization on the side-walls and in the bottom areas of the hole as described by Wu *et al*.[7,8] The coercivity of the patterned MO layer was found to be much higher than in the unpatterned MO layer (almost twice higher), moreover within the patterned area the coercivity was higher in the larger pinning sites than in the smaller pinning sites. The magnetic domains were found to be pinned inside the radial hole array and resembled the geometric shapes of the hole array. That the MFM images certainly reveal the magnetic pinned domains was verified by magnetizing and demagnetizing the sample with various magnetic field orientations relative to the film plane and field strength. Although we showed only radial hole array in this article, we have also observed that the magnetic domains could be pinned within the hole arrays with different types of geometry, such as square-, circle-, donut-, and star-shape. In principle, it is possible to fabricate any desired domain geometry with this technique. However, for pinning smaller domains, the present results indicate that the aspect ratio of the holes' dimension to the depth is critical. In addition, it was observed that the stability of the pinned domain is also affected by the sample's magnetization. Further work is necessary for the optimization of the MO recording media, such as the studies of changing the aspect ratio of the holes' dimension to the depth and the magnetization in thin film MO media.

Acknowledgment

We are grateful for the financial support by the National Science Council, the Republic of China, under grant of NSC88-2112-M-018-010.

1) M. A. M. Haast, J. R. Schuurhuis, L. Abelmann, J. C. Lodder and Th. J. Popma: IEEE Trans. Magn. **34** (1998) 1006.
2) M. Thielen, S. Kirsch, H. Weinforth, A. Carl and E. F. Wassermann: IEEE Trans. Magn. **34** (1998) 1009.
3) Te-ho Wu and M. Monsuripur: J. Magn. Soc. Jpn. **17S1** (1993) 131.
4) Y. Honda, N. Inaba, F. Tomiyama, T. Yamamoto and M. Futamoto: Jpn. J. Appl. Phys. **34** (1995) L987.
5) C. J. Lin and D. Rugar: IEEE Trans. Magn. **MAG-24** (1998) 2311.
6) S. Gadetsky, T. Suzuki, J. K. Erwin and M. Mansuripur: Proc. MORIS'94, J. Magn. Soc. Jpn. **19S1** (1995) 91.
7) Te-ho Wu, J. C. Wu, B. M. Chen and Han-Ping D. Shieh: J. Magn. Soc. Jpn. **22S2** (1998) 145.
8) Te-ho Wu, J. C. Wu, B. M. Chen and Han-Ping D. Shieh: IEEE Trans. Magn. **34** (1998) 1994.
9) A 30 kV of Hitachi S2460N SEM equipped with a versatile pattern generator is used for the structure fabrication in this study. The writing software, Nanopattern Generator Systems (NPGS), is produced by JC Nabity Lithography Systems, Bozeman, MT59717.
10) K. Babcock, M. Dugas, S. Manalis and V. Elings: Mater. Res. Soc. Symp. Proc. **335** (1995) 331.
11) K. Babcock, V. Elings, J. Shi, D. D. Acoschalom and M. Dugas: Appl. Phys. Lett. **69** (1996) 705.